

# Analysis of Single-Cell Transcriptome and Surface Protein Expression in Ankylosing Spondylitis Identifies OX40-Positive and Glucocorticoid-Induced Tumor Necrosis Factor Receptor-Positive Pathogenic Th17 Cells

Kijong Yi,<sup>1</sup> Sungsin Jo,<sup>2</sup> Woogil Song,<sup>3</sup> Hae-In Lee,<sup>4</sup> Hui-Ju Kim,<sup>4</sup> Ji-Hyoun Kang,<sup>4</sup> Seon Uk Kim,<sup>5</sup> Seung Hoon Lee,<sup>2</sup> Jinsung Park,<sup>2</sup> Tae-Hwan Kim,<sup>6</sup> Jeong Seok Lee,<sup>7</sup> Eun Young Lee,<sup>5</sup> and Tae-Jong Kim<sup>4</sup>

**Objective.** To demonstrate the immune landscape of blood and synovial cells in the setting of ankylosing spondylitis (AS) through the analysis of both single-cell transcriptome and surface protein expression, and to unveil the molecular characteristics of pathogenic Th17 cells.

**Methods.** This study included 40 individuals with active AS, 20 individuals with stable AS, 40 patients with active rheumatoid arthritis, and 20 healthy controls. Surface phenotype and intracellular staining were assessed using flow cytometry after peripheral blood mononuclear cells and synovial fluid mononuclear cells were stimulated with T cell receptor. Single-cell transcriptomes of 6 patients with active AS were studied along with cellular indexing of transcriptomes and epitopes by sequencing. We also assessed the outcome of targeting OX40 and glucocorticoid-induced tumor necrosis factor receptor (GITR) on the surface of Th17 cells in a mouse model of curdlan-injected SKG mice in which anti-GITR ligand and/or anti-OX40 ligand were used.

**Results.** We identified pathogenic Th17 cells as polyfunctional interleukin-17A (IL-17A)- and interferon- $\gamma$  (IFN $\gamma$ )-producing memory CD4+ T cells, with clinically supportive evidence for their pathogenic roles at sites of inflammation in AS. Transcriptome and flow cytometric analyses revealed that the coexpression of *TNFRSF4* (OX40) and *TNFRSF18* (GITR) is increased in pathogenic Th17 cells. Suppression of ligand receptor interactions in vivo through OX40 and GITR effectively suppressed clinical arthritis and decreased pathogenic Th17 cells in the curdlan-injected SKG mouse model.

**Conclusion.** Our results have implications for the understanding of pathogenic Th17 cells in AS patients and suggest potential therapeutic targets.

## INTRODUCTION

Interleukin-17 (IL-17) was identified and cloned from activated memory CD4+ T cells, which revealed a new type of

helper T cells called Th17 cells (1). As part of the adaptive immune system, a key role of Th17 cells is to mediate the clearance of fungal infections and extracellular pathogens through the promotion of granulopoiesis and the maintenance of mucosal barrier

Supported by the National Research Foundation of Korea (grant NRF-2021R111A3047818), the Chonnam National University Hospital Biomedical Research Institute (grant BCRI 21024), and the Chonnam National University (grant 2020-1764 awarded to Dr. T. J. Kim). Dr. T. H. Kim's work was supported by the National Research Foundation of Korea (grant NRF-2021R1A6A1A03038899). Dr. J. S. Lee's work was supported by the National Research Foundation of Korea (grants NRF-2022R1C1C1012634 and NRF-2022M3A9D3016848). Dr. E. Y. Lee's work was supported by the Ministry of Health and Welfare of the Republic of Korea (grant HI14C1277).

Drs. Yi and Jo and Mr. Song contributed equally to this work.

<sup>1</sup>Kijong Yi, MD, PhD: Genome Insight, San Diego, California; <sup>2</sup>Sungsin Jo, PhD, Seung Hoon Lee, PhD, Jinsung Park, PhD: Hanyang University Institute for Rheumatology Research (HYIRR), Seoul, Republic of Korea; <sup>3</sup>Woogil Song, BS: Graduate School of Medical Science and Engineering, Korea Advanced Institute of Science and Technology, Daejeon, Republic of Korea; <sup>4</sup>Hae-In Lee, MS, Hui-Ju Kim, MS, Ji-Hyoun Kang, MD, PhD, Tae-Jong Kim, MD, PhD:

Department of Rheumatology, Chonnam National University Medical School and Hospital, Gwangju, Republic of Korea; <sup>5</sup>Seon Uk Kim, MS, Eun Young Lee, MD, PhD: Division of Rheumatology, Department of Internal Medicine, Seoul National University College of Medicine, Seoul, Republic of Korea; <sup>6</sup>Tae-Hwan Kim, MD, PhD: Hanyang University Institute for Rheumatology Research and Department of Rheumatology, Hanyang University Hospital for Rheumatic Diseases, Seoul, Republic of Korea; <sup>7</sup>Jeong Seok Lee, MD, PhD: Genome Insight, San Diego, California, and Graduate School of Medical Science and Engineering, Korea Advanced Institute of Science and Technology, Daejeon, Republic of Korea.

Author disclosures and a graphical abstract are available online at <https://onlinelibrary.wiley.com/doi/10.1002/art.42476>.

Address correspondence via email to Jeong Seok Lee, MD, PhD, at [chemami@kaist.ac.kr](mailto:chemami@kaist.ac.kr); to Eun Young Lee, MD, PhD, at [elee@snu.ac.kr](mailto:elee@snu.ac.kr); or to Tae-Jong Kim, MD, PhD, at [ktj1562@jnu.ac.kr](mailto:ktj1562@jnu.ac.kr).

Submitted for publication April 29, 2022; accepted in revised form February 7, 2023.

functions (2–4). In addition, Th17 cells play critical roles in the pathogenesis of chronic inflammatory diseases, including experimental allergic encephalomyelitis, psoriasis, uveitis, inflammatory bowel disease, and ankylosing spondylitis (AS) (2,5–9).

AS is a chronic, immune-mediated rheumatic disease characterized by inflammation of the axial skeleton, peripheral joints, and heterogeneous extramusculoskeletal manifestations such as bowel inflammation, psoriasis, and uveitis (10). Various immune cells have been reported to play important roles in the initiation and progression of AS, and there is strong evidence implicating Th17 in the pathogenesis of AS. An increased frequency of Th17 cells is a hallmark of AS (9), and these cells appear to be functionally important, as has been indicated by the therapeutic response to IL-17A neutralization (11).

Although Th17 cells have been involved in the induction of inflammation, using an IL-17A blocker to treat patients with inflammatory bowel disease has resulted in disease aggravation (12). Moreover, antibody therapies targeting IL-17A have been ineffective for bowel inflammation or uveitis in AS (13,14), in contrast to the marked effectiveness for psoriasis (15,16). However, emerging data suggest that not all Th17 cells are pathogenic. Th17 cells can either cause severe tissue damage or have no effect on inducing autoimmune diseases (17,18). Therefore, ongoing studies have focused on defining the characteristics of pathogenic Th17 cells.

Cells producing both IL-17 and interferon- $\gamma$  (IFN $\gamma$ ) have been reported to be the main pathogenic Th17 cells that induce inflammation in the joints or gut (19,20). CD161+ Th17 cells are enriched at sites of joint inflammation and appear to be pathogenic (21). When comparing gene expression profiles between pathogenic Th17 cells and nonpathogenic Th17 cells, pathogenic Th17 cells express more effector molecules, including proinflammatory cytokines and chemokines such as CXCL3, CCL4, CCL5, IL-3, and IL-22, and transcription factors such as TBX2 and STAT4 (18,22).

However, the majority of data from recent studies were derived from in vitro cell differentiation or isolated mouse tissues. Therefore, we tried to map the cellular landscape of blood and synovial cells from AS patients through both single-cell transcriptome and surface protein expression analyses, focusing on pathogenic Th17 cells. Here, we identify *TNFRSF4* (OX40) and *TNFRSF18* (glucocorticoid-induced tumor necrosis factor receptor [GITR]) double-positive T helper cells as pathogenic Th17 cells in AS synovial tissue that are associated with disease activity. These findings have implications in our understanding of pathogenic Th17 cells in AS and suggest potential therapeutic targets.

## PATIENTS AND METHODS

This study cohort included AS patients who satisfied the modified New York criteria for AS (23), as well as rheumatoid arthritis (RA) patients and healthy controls. The clinical characteristics of the subjects are summarized in Table 1. The investigation was carried out in compliance with the Helsinki Declaration and was approved by the ethics committee of Chonnam National University Hospital (CNUH). Written informed consent was obtained from all participants (institutional review board [IRB] no. CNUH-2011-199).

**Flow cytometry and enzyme-linked immunosorbent assay.** Peripheral blood mononuclear cells (PBMCs) and synovial fluid mononuclear cells (SFMCs) were isolated and suspended in a complete medium (RPMI 1640 medium, 2 mM L-glutamine, 100 units/ml of penicillin, and 100 mg/ml of streptomycin) supplemented with 10% fetal bovine serum (Gibco BRL) and seeded in 96-well plates at a cell density of  $1 \times 10^6$  cells/well. The cells were surface-stained with anti-Fixable Viability Dye eFluor 780, Pacific Blue anti-CD4, PE anti-CD45RO, Brilliant Violet 711 anti-OX40/APC anti-GITR, or APC anti-OX40/PerCP/Cy5.5 anti-GITR (all from BioLegend). Cells were washed, fixed, permeabilized with Cytofix/Cytoperm buffer, intracellularly stained with antibodies

**Table 1.** Clinical characteristics of healthy controls and patients with ankylosing spondylitis (AS) or rheumatoid arthritis (RA)\*

	PBMCs				SFMCs	
	Healthy controls (n = 20)	AS stable (n = 20)	AS active (n = 20)	RA active (n = 20)	AS active (n = 40)	RA active (n = 40)
Age, mean $\pm$ SD years	31.8 $\pm$ 10.4	36.4 $\pm$ 11.3	34.6 $\pm$ 11.5	58.8 $\pm$ 13.8	34.6 $\pm$ 12.4	59.5 $\pm$ 11.9
Male	16 (80)	13 (65)	14 (70)	5 (25)	26 (65)	6 (15)
BASDAI score, mean $\pm$ SD	NA	2.19 $\pm$ 2.47	6.17 $\pm$ 2.20	NA	7.13 $\pm$ 2.25	NA
ASDAS, mean $\pm$ SD	NA	1.65 $\pm$ 0.81	4.11 $\pm$ 1.15	NA	3.33 $\pm$ 1.83	NA
CRP level, mean $\pm$ SD mg/dl	NA	0.12 $\pm$ 0.10	3.56 $\pm$ 2.96	4.14 $\pm$ 3.48	6.39 $\pm$ 5.88	2.50 $\pm$ 2.55
HLA-B27-positive	NA	20 (100)	20 (100)	NA	40 (100)	NA
Current treatments						
NSAID	NA	16 (80)	20 (100)	19 (95)	40 (100)	21 (52.5)
Sulfasalazine	NA	4 (20)	15 (75)	3 (15)	35 (87.5)	5 (12.5)
TNF blocker	NA	6 (30)	8 (40)	2 (10)	19 (47.5)	3 (7.5)
IL-17 blocker	NA	0 (0)	0 (0)	0 (0)	0 (0)	0 (0)

\* Except where indicated otherwise, values are the number (%) of patients. PBMCs = peripheral blood mononuclear cells; SFMCs = synovial fluid mononuclear cells; BASDAI = Bath Ankylosing Spondylitis Disease Activity Index; NA = not applicable; ASDAS: Ankylosing Spondylitis Disease Activity Score; CRP = C-reactive protein; NSAID = nonsteroidal antiinflammatory drug; TNF = tumor necrosis factor; IL-17 = interleukin-17.

against IFN $\gamma$  (fluorescein isothiocyanate)/IL-17A (allophycocyanin), or IFN $\gamma$  (allophycocyanin Alexa Fluor 700)/IL-17A (fluorescein isothiocyanate) and analyzed. For intracellular cytokine staining, samples were stimulated with Dynabeads Human T-Activator CD3/CD28 (product no. 11131D; Gibco) to obtain a bead-to-cell ratio of 1:1. The levels of cytokines (IFN $\gamma$ , IL-17A, IL-23, and IL-6, purchased from Invitrogen) and tumor necrosis factor (TNF) superfamily ligand (OX40 ligand [OX40L] and GITR ligand [GITRL], purchased from R&D systems) in the serum or synovial fluid (SF) were assessed using enzyme-linked immunosorbent assays, according to the manufacturer's instructions.

#### Single-cell RNA sequencing of PBMCs and SFMCs.

PBMCs and SFMCs were isolated from 6 AS patients using a Ficoll gradient separation technique. Single-cell RNA sequencing, cellular indexing of transcriptomes and epitopes by sequencing (CITE-seq), and single-cell T cell receptor sequencing libraries were generated using the Chromium system (Chromium Next GEM Single Cell 5' Kit v.1, 5' Feature Barcode Kit, and Chromium Single Cell Human TCR Amplification Kit, all from 10x Genomics). We used cell multiplexing and 3 samples were processed by a single gel bead in emulsion (GEM) at once and demultiplexed by genotype for donors 1, 2, 3, and 4 (24). SFMC samples from donors 5 and 6 were processed separately by each GEM, and PBMC samples from donors 5 and 6 were processed by a single GEM and demultiplexed by genotype. Libraries were sequenced using the Illumina Novaseq 6000 system. All data were processed by cellranger version 3.0.2 and manipulated and visualized using R version 4.1.1 and Seurat version 4.0.2. Batch correction was performed to integrate single-cell data from all 6 donors using Harmony (25). The code for downstream analysis is available at <https://github.com/kijong-yi/as>. Enrichment analysis for portion-specific genes and ligand perturbation-responsive genes was performed using Enrichr (26,27).

Clonotype assembly of single-cell T cell receptor (TCR) data was performed with the "vdj" command of the cellranger software according to its instruction guide. We used the ImMunoGene Tics database for assembly and clonotype annotation. Cell barcodes were typed as "Orphan," "Expanded (2)," or "Expanded (>2)," based on the number of cells in each clonotype. The cell barcodes that do not appear in the TCR data set but exist only in gene expression data were represented as "No information." The cell barcodes without single-cell gene-expression data were omitted in the clonotyping.

#### Murine disease model, intervention, and scoring.

SKG mice on a BALB/c background were purchased from CLEA Japan. All experiments were approved by the Institutional Animal Care and Use Committee (animal experiment IRB nos. CNU IACUC-H-2020-14 and CNU IACUC-H-2022-32) and conducted in accordance with the Laboratory Animals Welfare Act Guide for the Care and Use of Laboratory Animals. Eight-week-old female mice were treated with curdlan (3 mg/kg) by intraperitoneal injection. The following week, curdlan-injected mice were randomly

stratified into 4 groups and treated weekly for 5 weeks with 1  $\mu$ g of anti-mouse GITRL (product no. MAB2177; R&D Systems) and/or 1  $\mu$ g of anti-mouse OX40L (product no. BE0033-1; Bio X Cell) via tail vein injection. We used 1  $\mu$ g of IgG (product no. I4506; Sigma) as control. Arthritis scoring and ankle thickness were observed and measured weekly. Clinical arthritis scores were evaluated by 2 independent observers. The scores of the affected joints were summed as described in a previous report (28).

**Tissue preparation and histologic staining.** For histology, ankles were fixed in 10% formalin for 2–3 days at room temperature and decalcified with 10% formic acid for 1 week with shaking. The decalcified specimens were embedded in paraffin and sectioned (5–6  $\mu$ m thick) for hematoxylin and eosin (H&E) staining. Whole H&E images of ankle specimens were digitally scanned by axioscan 7. Histopathologic findings at the ankle were scored according to a previous report (28).

**Immunofluorescent staining.** The section slides were deparaffinized in Neo-Clear and rehydrated in serial ethanol, followed by antigen retrieval with proteinase K (ab64220; Abcam) at room temperature for 30 minutes and blocking with BLOXALL (SP-6000; Vector) for 1 hour. To observe the colocalization of CD4, IL-17A, and IFN $\gamma$ , the slides were incubated with primary mouse antibody for CD4 at a dilution of 1:100 (catalog no. sc-19641; Santa Cruz Biotechnology), rabbit antibody for IL-17A at a dilution of 1:100 (ab79056; Abcam), and rat antibody for IFN $\gamma$  at a dilution of 1:100 (product no. 16-7311-81; Invitrogen) at room temperature for 1 hour, followed by incubation with Alexa Fluor 488–conjugated anti-mouse antibody at a dilution of 1:200 (product no. A11001; Invitrogen), Cy3-Alexa–conjugated anti-rabbit antibody at a dilution of 1:100 (product no. 111-165-144; Jackson ImmunoResearch), and Cy5-conjugated anti-rat antibody at a dilution of 1:200 (product no. 712-175-153; Jackson ImmunoResearch) at room temperature for 1 hour. To avoid nonspecific staining, the stained slides were treated with DAPI using the Autofluorescence Quenching kit (product no. SP-8500; Vector). Images of immunofluorescent stains were collected by a confocal microscope (Leica Microsystem). The number of colocalized cells in each specimen was counted in visual fields without nonspecific signals. Average values were determined by 2 independent observers.

**Data availability.** All raw and processed data have been deposited in the GEO database under accession number GSE 216885.

## RESULTS

**Increase in polyfunctional Th17 cells in SF of patients with AS and association with higher disease activity.** Using intracellular staining, we analyzed the frequency of IL-17A– and IFN $\gamma$ –producing memory CD4+ T cells in PBMC

and SFMC samples from AS and RA patients with active or stable disease, and in PBMC samples from healthy controls (Figure 1A, Table 1, and Supplementary Figure 1A, <http://onlinelibrary.wiley.com/doi/10.1002/art.42476>). The frequency of memory CD4+ T cells, defined by CD45RO positivity, was significantly higher in the SFMC samples than in the PBMC samples from patients with AS or RA (Supplementary Figure 1B).

As has also been shown in previous studies (29), we observed strong activation of Th17 cells in patients with AS, especially in the involved joints. PBMCs from patients with active AS had a significantly higher frequency of IL-17A+ cells among memory CD4+ T cells as compared to healthy controls (Figure 1B). In addition, the frequency of IL-17A+ cells among SFMCs from patients with active AS was increased compared to those from

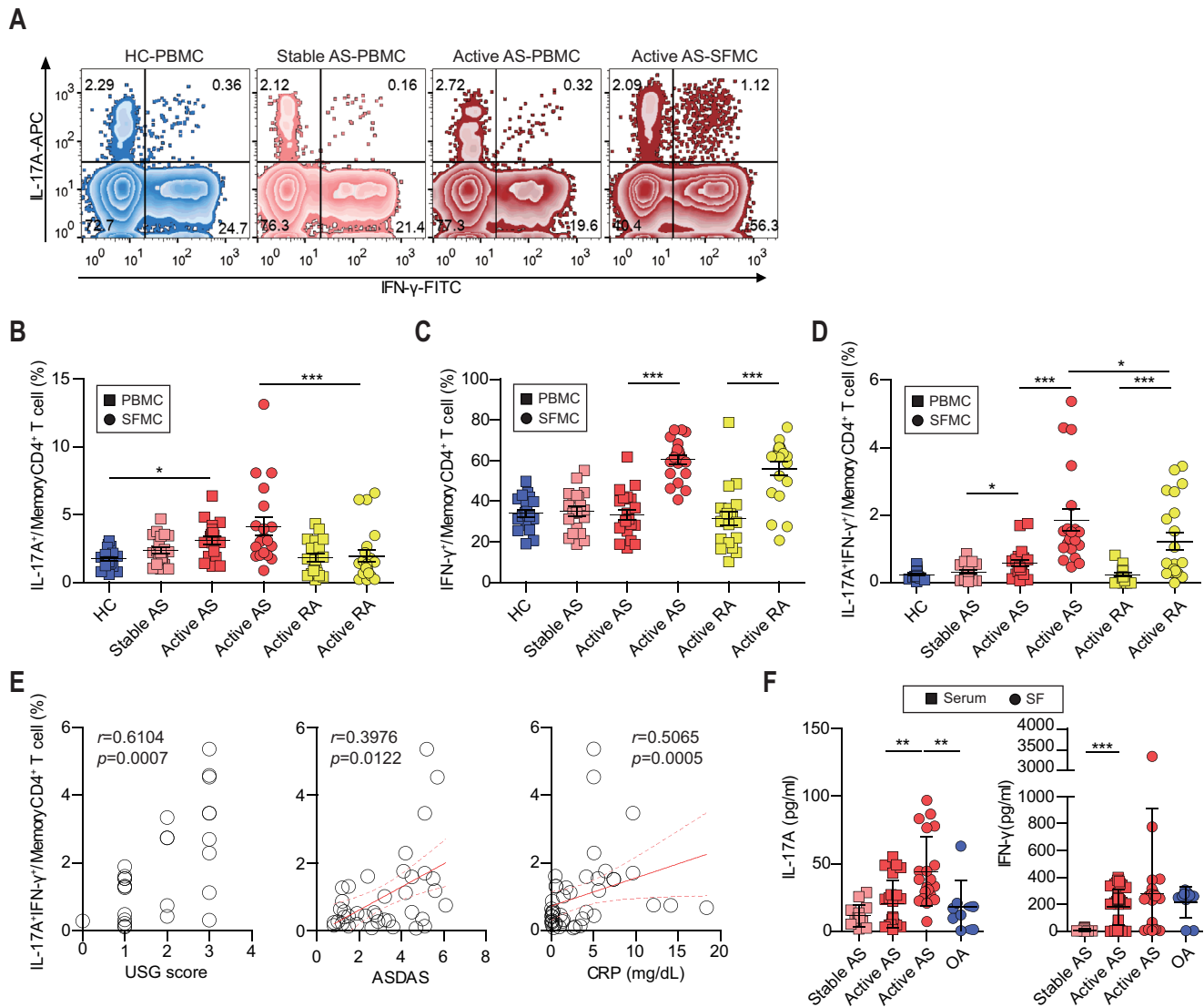


**Figure 1.** Polyfunctional pathogenic Th17 cells in synovial fluid and peripheral blood immune cells. **A–E**, After intracellular staining, flow cytometry was used to measure proportions of interleukin-17A (IL-17A)– and interferon- $\gamma$  (IFN $\gamma$ )–secreting memory CD4+ T cells in peripheral blood mononuclear cell (PBMC) or serum samples from healthy controls (HCs) ( $n = 20$ ), patients with stable ankylosing spondylitis (AS) ( $n = 20$ ), patients with active AS ( $n = 20$ ), and patients with active rheumatoid arthritis (RA) ( $n = 20$ ), and in synovial fluid mononuclear cell (SFMC) or synovial fluid (SF) samples from patients with AS ( $n = 40$ ), patients with RA ( $n = 40$ ), or patients with osteoarthritis (OA) ( $n = 10$ ). **A**, Representative contour plots showing PBMCs from HCs and from AS patients with stable or active disease and SFMCs from AS patients with active disease. **B–D**, Proportions of IL-17A+, IFN $\gamma$ +, and IL-17A+IFN $\gamma$ + cells among memory CD4+ T cells in PBMC samples from HCs, patients with stable AS, patients with active AS, and patients with active RA, or SFMC samples from patients with AS and patients with RA. **E**, Correlations between proportions of IL-17A+IFN $\gamma$ + memory CD4+ T cells and clinical parameters including ultrasonographic (USG) score, Ankylosing Spondylitis Disease Activity Score (ASDAS), and serum C-reactive protein (CRP) levels (Spearman's correlation coefficient was used). **F**, Soluble protein level of IL-17A and IFN $\gamma$  in the synovial fluid or serum of patients with AS or OA as measured by enzyme-linked immunosorbent assay. Symbols represent individual samples. \* =  $P < 0.05$ ; \*\* =  $P < 0.005$ ; \*\*\* =  $P < 0.0005$ . APC = allophycocyanin.

patients with active RA. For IFN $\gamma$ -producing cells among memory CD4<sup>+</sup> T cells, SFMCs had a higher frequency than corresponding PBMCs in patients with AS or RA (Figure 1C). However, the frequency of IFN $\gamma$ <sup>+</sup> cells was not significantly different between the

SFMCs from AS and RA patients. Intriguingly, simultaneous production of both IL-17A and IFN $\gamma$  by memory CD4<sup>+</sup> T cells was increased in the SFMCs from AS patients as compared to those from RA patients, like IL-17A<sup>+</sup> memory CD4<sup>+</sup> cells. A higher

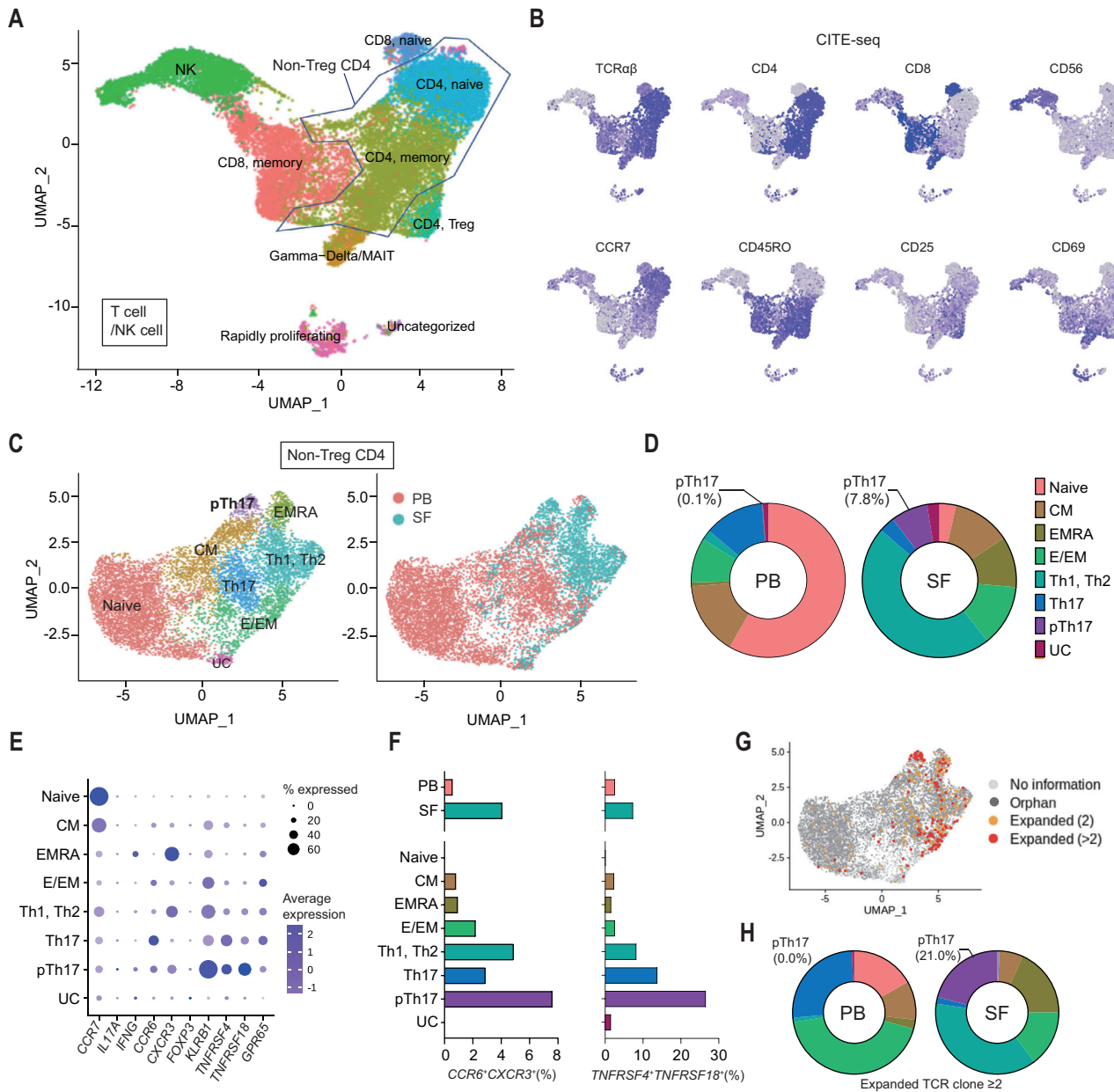


**Figure 2.** Specific subclusters expressing key features of pathogenic Th17 (pTh17) cells in SFMC samples from AS patients. **A**, Subclusters of T cells and natural killer (NK) cells among the initial 8 cell clusters that originated from PBMC–SFMC pairs from patients with AS ( $n = 6$ ). **B**, Surface protein expression (assessed using cellular indexing of transcriptomes and epitopes by sequencing) of 8 representative antigens for which the following antibodies were used: TotalSeq anti-human antibodies for T cell receptor  $\alpha\beta$  (TCR  $\alpha\beta$ ), CD4, CD8, CD56, CD197, CD45RO, CD25, and CD69. For proper contrast in display, we adjusted color scale by adding optional parameter (min.cutoff = ‘q9’ at FeaturePlot function in Seurat software). **C**, Subclusters of “Non-Treg CD4” cells among the 9 T cell/NK cell–originated subclusters (left); subclusters originating from peripheral blood (PB) and SF marked in red and blue, respectively (right). **D**, Proportions of each subcluster among non-Treg CD4 cells according to PB and SF origin. **E**, Expression levels of 10 genes associated with Th1, Th17, and pTh17 cells. **F**, Frequency of double-positive cells evaluated by the presence of transcripts *CCR6* and *CXCR3* or *TNFRSF4* and *TNFRSF18*. **G**, Clonality of TCRs presented on the Uniform Manifold Approximation and Projection (UMAP) of “Non-Treg CD4” cells. **H**, Proportions of each subcluster among clonally expanded non-Treg CD4 cells; clonal expansion defined by the number of TCR sequences (2 or more). See Figure 1 for other definitions.

frequency of memory CD4<sup>+</sup> T cells produced IL-17A and IFN $\gamma$  in SFMCs than PBMCs from patients with AS or RA (Figure 1D).

The frequency of polyfunctional IL-17A<sup>+</sup> and IFN $\gamma$ -producing memory CD4<sup>+</sup> T cells was associated with clinical parameters, including power doppler signal score measured from synovial ultrasonography (30), Ankylosing Spondylitis Disease Activity Score (ASDAS) (31), and serum level of C-reactive protein (Figure 1E). The frequency of IL-17A<sup>+</sup> memory CD4<sup>+</sup> T cells was positively associated with only the ultrasonography score and the ASDAS. (Supplementary Figure 1C, <http://onlinelibrary.wiley.com/doi/10.1002/art.42476>). The frequency of IFN $\gamma$ <sup>+</sup> memory CD4<sup>+</sup> T cells did not show a significant correlation with clinical parameters (Supplementary Figure 1D). Therefore, polyfunctional IL-17A<sup>+</sup>IFN $\gamma$ <sup>+</sup> memory CD4<sup>+</sup> T cells in SF samples from patients with AS were associated with higher disease activity.

Because Th17 cells exhibit a high degree of plasticity, we measured the cytokine milieu in SF samples from patients with AS and compared it to that of patients with osteoarthritis (OA). The level of IL-17A was significantly higher in SF samples from patients with AS than in the serum of patients with AS and the SF of patients with OA (Figure 1F, left). In contrast, levels of IFN $\gamma$  in SF samples from patients with active AS were not remarkably different from levels in the serum of patients with AS or the SF samples of patients with OA (Figure 1F, right). The increased level of IL-6 with further exposure to IL-23 drives the differentiation of pathogenic Th17 cells (18). In this study, the finding of higher levels of IL-6 and IL-23 in SF samples may support the idea that inducing pathogenic Th17 cells causes joint inflammation in individuals with AS (Supplementary Figure 1E, <http://onlinelibrary.wiley.com/doi/10.1002/art.42476>). In summary, we identified polyfunctional IL-17A<sup>+</sup> and IFN $\gamma$ -producing memory CD4<sup>+</sup> T cells in patients with AS, as well as clinical evidence of their pathogenic role at the site of inflammation.

**Comparative single-cell landscape of PBMCs and SFMCs from patients with active AS.** To profile the immune landscape of AS, we performed single-cell transcriptome analysis of PBMC and SFMC samples simultaneously obtained from patients with AS (n = 6). Using a 10x Genomics platform, we analyzed a total of 45,106 cells after filtering dead cells and doublets. We detected an average of 5,694 unique molecular identifiers and 1,645 genes per cell. Analyzing 45,106 cells with a uniform manifold approximation and projection algorithm based on variable genes with the Seurat package (32), we identified 10 clusters. After the initial clustering, we annotated 8 different cell types expressing representative marker genes: B cells, peripheral blood monocytes, natural killer cells, uncategorized cells, plasmacytoid dendritic cells, dendritic cells, SF monocytes, and T cells (Supplementary Figures 2A and B and Supplementary Table 1, <http://onlinelibrary.wiley.com/doi/10.1002/art.42476>). Surface protein expression measured by CITE-seq confirmed the annotated cell types (Supplementary Figure 2C) (33). The absolute cell

count of each cell type in the individual samples showed that the majority of SF cells were monocytes and T cells (Supplementary Figure 2D).

**Identification of a subcluster as potentially pathogenic SFMC-specific Th17 cells.** To identify pathogenic Th17 cells among similar populations of memory CD4<sup>+</sup> T cells, an additional subclustering analysis of T cells and natural killer cells among the initial 8 clusters was performed. Next, we annotated 9 different cell types expressing representative marker genes: memory CD4 cells, naive CD4 cells, Treg cells, memory CD8 cells,  $\gamma\delta$ T cells/mucosal-associated invariant T cells, natural killer cells, rapidly proliferating cells, and uncategorized cells (Figure 2A, and Supplementary Figure 2E and Supplementary Table 2, <http://onlinelibrary.wiley.com/doi/10.1002/art.42476>). Surface protein expression measured by CITE-seq confirmed the expression of T cell receptor  $\alpha\beta$ , CD4, CD8, CD56, CCR7, CD45RO, CD25, and CD69 according to the assigned cell types (BioLegend antibody category nos. 306737, 344651, 344753, 392425, 353251, 304259, 302649, and 310951, respectively). (Figure 2B).

With the clusters including CD4<sup>+</sup> T cells, except for Treg cells, we performed the third clustering analysis to determine the known features of pathogenic Th17 cells (Figure 2C). We annotated 8 different cell types expressing representative markers: naive cells, central memory cells, effector memory RA cells, effector and/or effector memory cells, Th1 and Th2 cells, Th17 cells, pathogenic Th17 cells, and uncategorized clusters (Figures 2C and D and Supplementary Table 3, <http://onlinelibrary.wiley.com/doi/10.1002/art.42476>). Intriguingly, pathogenic Th17 cells had evident simultaneous up-regulation of *KLRB1* (CD161) and *GPR65*, which are known as markers of pathogenic Th17 cells (22).

The proportion of pathogenic Th17 cells among non-Treg CD4 T cells was higher in SF (7.8%) than in peripheral blood (0.1%) (Figure 2D). Pathogenic Th17 cells overexpressed both *CCR6* and *CXCR3*, which is characteristic of memory CD4<sup>+</sup> T cells with Th17 and Th1 cell types, respectively (Figures 2E and F, left). Among the other markers of pathogenic Th17 cells (Supplementary Table 3, <http://onlinelibrary.wiley.com/doi/10.1002/art.42476>), *TNFRSF4* (OX40) and *TNFRSF18* (GITR) were markedly increased in both Th17 and pathogenic Th17 cells (Figure 2E). Among 8 subclusters of non-Treg CD4 T cells, pathogenic Th17 cells had the highest frequency of cells with coexpressed OX40 and GITR (Figure 2F, right). OX40 and GITR are cell-surface proteins that are members of the TNF receptor superfamily, and are targeted by antagonistic or agonistic antibodies in inflammatory disease or cancer (34–39).

Evaluating TCR clonality provides an understanding of the potential expansion of autoantigen-reactive T cells (Figure 2G). Clonally expanded pathogenic Th17 cells, which had 2 or more expanded TCR clones, were observed only in the SF (21.0%), as

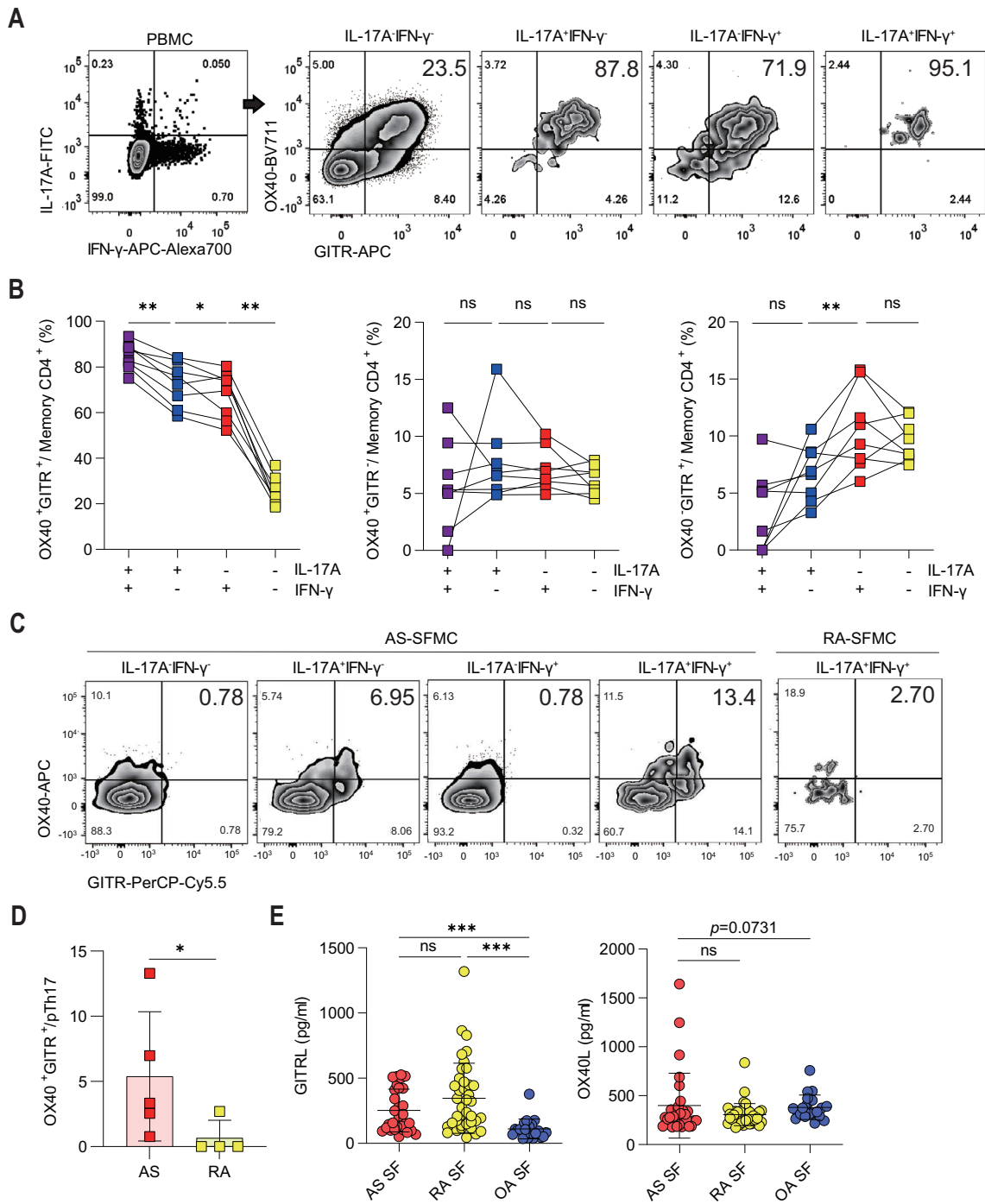


**Figure 3.** OX40 and glucocorticoid-induced tumor necrosis factor receptor (GITR) as specific markers of pathogenic Th17 cells. **A**, Gating strategy to examine the correlation between IL-17/IFN $\gamma$  and OX40/GITR among memory CD4 $^{+}$  T cells. Cell surfaces were stained with anti-OX40 and anti-GITR, and cells were intracellularly stained with antibodies against IFN $\gamma$ /IL-17A and analyzed. For intracellular cytokine staining, samples were stimulated with Dynabeads Human T-Activator CD3/CD28. **B**, Frequency of OX40+GITR $^{+}$ , OX40-GITR $^{-}$ , and OX40-GITR $^{+}$  cells in IL-17+IFN $\gamma$  $^{+}$ , IL-17+IFN $\gamma$  $^{-}$ , IL-17-IFN $\gamma$  $^{+}$ , and IL-17-IFN $\gamma$  $^{-}$  memory CD4 $^{+}$  T cells ( $n = 8$ ). **C**, Expression levels of OX40 and GITR among memory CD4 $^{+}$  T cells based on expression of IL-17A and IFN $\gamma$  in the SFMCs of patients with AS and patients with RA. **D**, Frequency of OX40+GITR $^{+}$  cells among IL-17+IFN $\gamma$  $^{+}$  (pathogenic Th17) cells among the SFMCs of patients with AS ( $n = 5$ ) and patients with RA ( $n = 4$ ). **E**, Soluble protein concentration of GITR ligand (GITRL) and OX40L in the SF of patients with AS ( $n = 30$ ), patients with RA ( $n = 40$ ), and patients with OA ( $n = 20$ ). \* =  $P < 0.05$ ; \*\* =  $P < 0.005$ ; \*\*\* =  $P < 0.0005$ . FITC = fluorescein isothiocyanate; ns = not significant (see Figure 1 for other definitions).

they were absent in the peripheral blood (Figure 2H). In summary, we found specifically SFMC-expanded, non-Treg, and memory type CD4<sup>+</sup> T cell subpopulations expressing the markers of pathogenic Th17 cells with clonal expansion in patients with AS.

**OX40 and GITR double-positivity as a specific surface marker for pathogenic Th17 cells in AS.** Next, we performed in vitro experiments to validate the association between the surface expression level of OX40/GITR and the

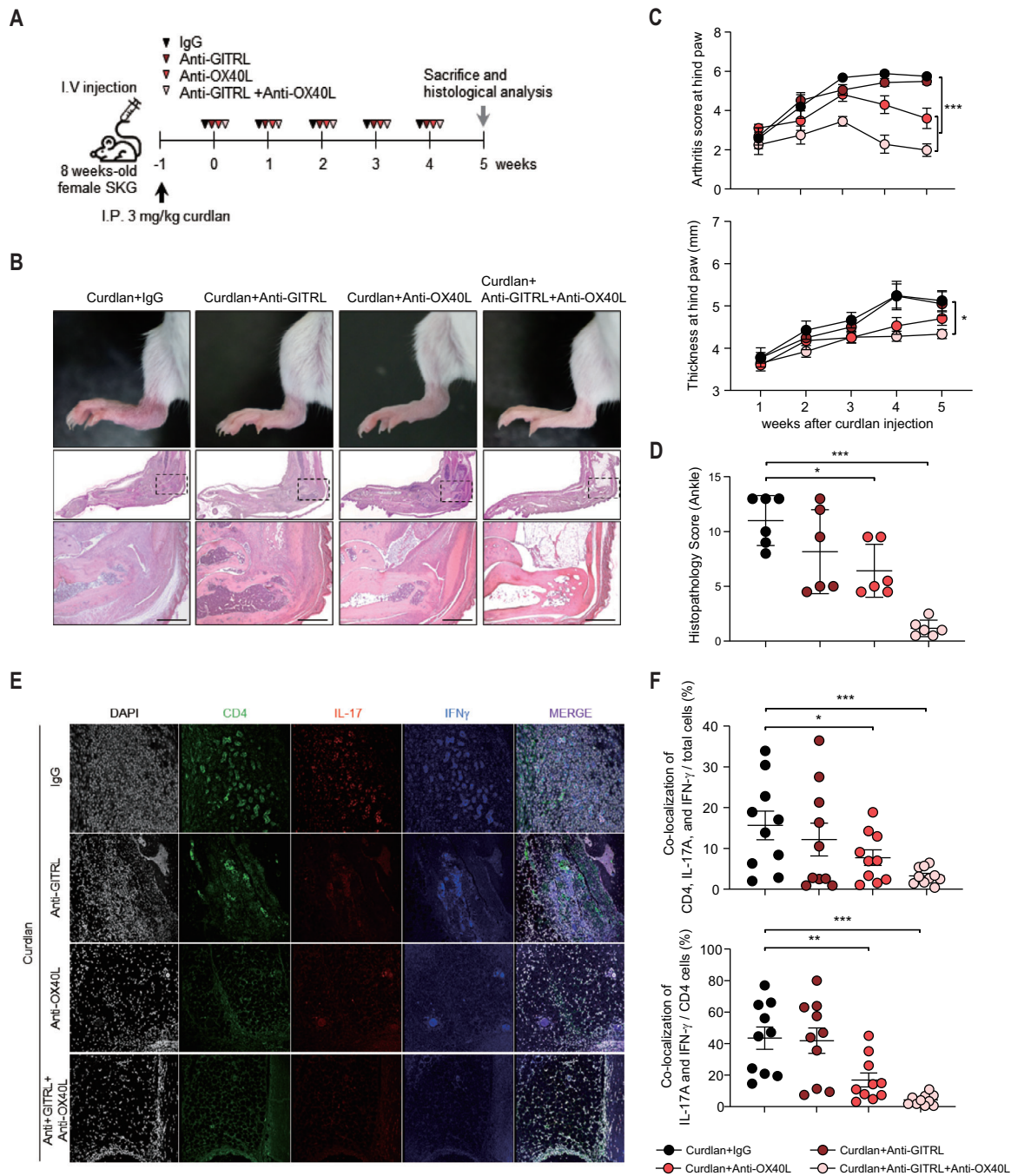


**Figure 4.** OX40 and glucocorticoid-induced tumor necrosis factor receptor (GITR) as therapeutic targets of pathogenic Th17 cells. **A**, Schematic timeline of experimental design in 8-week-old female SKG mice. **B**, Representative pictures (upper panel), whole hematoxylin and eosin (H&E) staining (middle panel), and 200 $\times$  magnification H&E staining (lower panel) of clinical arthritis features at the ankle in curdalan-treated female SKG mice treated with IgG, anti-GITR ligand (anti-GITRL), anti-OX40L, or anti-GITRL/anti-OX40L. **C**, Clinical arthritis scores and thickness in the hind paw were assessed ( $n = 6$  mice for each group). **D**, The mean histopathologic score of each mouse was measured at 5 weeks after curdalan injection. **E**, Immunostaining of CD4 (green), IL-17 (red), and IFN $\gamma$  (blue); nuclei were stained with DAPI (gray). **F**, Comparative analysis of cells expressing both IL-17 and IFN $\gamma$  by group using fluorescent confocal microscopy. Symbols represent stain data from individual ankles. \* =  $P < 0.05$ ; \*\* =  $P < 0.005$ ; \*\*\* =  $P < 0.0005$ . See Figure 1 for other definitions.



production of IL-17/IFN $\gamma$ . Flow cytometric analysis of human PBMC samples with anti-CD3/CD28 stimulation showed that the frequency of OX40+GITR+ copositive memory CD4+ T cells was >80% and significantly higher in IL-17+IFN $\gamma$ + cells than in IL-17 or IFN $\gamma$  single-positive cells (Figures 3A and B). However, the frequency of OX40 single-positive cells or GITR single-positive cells did not exhibit the pattern of OX40+GITR+ cells. By reversing the gating strategy, we compared the frequency of IL-17+IFN $\gamma$ + cells based on the patterns of OX40 and GITR expression (Supplementary Figure 3A, <http://onlinelibrary.wiley.com/doi/10.1002/art.42476>). OX40+GITR+ cells were associated with significantly increased IL-17+IFN $\gamma$ + cells among memory CD4+ T cells (Supplementary Figure 3B). Therefore, polyfunctional pathogenic Th17 cells have an increased frequency of OX40+GITR+ cells.

To validate the OX40/GITR expression patterns of TCR-stimulated PBMCs, we performed flow cytometric analysis in SFMCs from AS patients ( $n = 5$ ) and RA patients ( $n = 4$ ). The frequency of OX40+GITR+ copositive memory CD4+ T cells was highest in IL-17+IFN $\gamma$ + cells (Figure 3C). The OX40+GITR+ copositive frequency among pathogenic Th17 cells was significantly higher in SFMC samples from AS patients than in those from RA patients (Figure 3D). Therefore, coexpression of OX40 and GITR on the surface of memory CD4+ T cells would be a useful cellular marker and a treatable target of pathogenic Th17 cells. In addition, soluble GITRLs in SF samples were significantly elevated in AS and RA patients as compared to OA patients (Figure 3E, left). The level of OX40L tended to be increased in SF samples from AS patients compared to samples from OA patients ( $P = 0.0731$ ; Figure 3E, right).

**OX40 and GITR double-positive cells as a therapeutic target for pathogenic Th17 cells in an animal model.** We also assessed the outcome of targeting OX40 and GITR on the cell surface of Th17 cells in an in vivo model. We used the curdlan-injected SKG mouse model, a relevant in vivo model of AS for Th17 cell-dependent arthritis (40–42), and treated the experimental groups with anti-GITRL and/or anti-OX40L (Figure 4A). Mice that received treatment targeted for both GITRL and OX40L showed marked amelioration of clinical arthritis scores, thickness in the hind paw, and histologic arthritis scores of the ankle joint compared to control mice that received IgG (Figures 4B–D). Mice receiving single treatment with anti-GITRL did not show significant reductions in arthritis scores or thickness at the hind paw. Mice receiving anti-OX40L single treatment also had reduced arthritis scores at the hind paw and reduced histologic scores at the ankle (Figures 4C and D).

To confirm whether OX40 and GITR are the direct target of pathogenic Th17 cells in an in vivo experiment, pathogenic Th17 cells were observed under a confocal microscope after blocking OX40L and GITRL. Among total cells, cells expressing both IL-17A and IFN $\gamma$  were significantly increased in the ankle joint

tissues of control SKG mice (Figures 4E and F). Although the number of cells coexpressing IL-17A and IFN $\gamma$  was decreased in the anti-OX40L single-treatment group compared to the IgG-treated control group, the greatest decrease in coexpressing cells was found in the group treated with anti-GITRL and anti-OX40L. Along the same lines, the percentage of IL-17A and IFN $\gamma$  coexpression among CD4+ T cells was significantly decreased in the ankle joints of mice treated with anti-OX40L only and those cotreated with anti-GITRL and anti-OX40L, as compared to control mice. In summary, we found that cosuppression of OX40L and GITRL using antagonistic antibodies could be an effective treatment strategy by targeting pathogenic Th17 cells in arthritis.

## DISCUSSION

In the present study, single-cell transcriptome analysis using TCR profiling and protein expression (CITE-seq) demonstrated pathogenic Th17 cells expressing polyfunctional features (IL-17A+IFN $\gamma$ +) with the previously known transcriptomic features (such as *GPR65* and *KLRB1*) in the joint fluid of patients with AS. We found that OX40 and GITR are targetable molecules specifically expressed on the surface of pathogenic Th17 cells, and that pathogenic Th17 cells were decreased in the in vivo model by neutralization.

Plastic features of Th17 cells originate from the natural instability of retinoic acid receptor-related orphan nuclear receptor  $\gamma$  (ROR $\gamma$ )-associated positive feedback loops to maintain the function of Th17 cells (43). The cytokine milieu at sites of inflammation affects the Th17 differentiation program, and IFN $\gamma$ -expressing Th17 cells are known by several different names, including ex-Th17, Th17.1, and pathogenic Th17 cells (44,45). Most of the evidence linking plastic/polyfunctional Th17 cells to pathogenicity originates from in vivo studies, mainly studies of experimental allergic encephalomyelitis as an animal model of multiple sclerosis (18,22). However, proving the pathogenicity of a certain cell population in patients is difficult. In the present study, we suggested that a subpopulation of memory CD4+ T cells was pathogenic because of a positive correlation between pathogenic Th17 cell frequency and clinical parameters (ultrasonography score, ASDAS, and C-reactive protein level), known features of pathogenic Th17 cells shared by previous studies, the presence of pathogenic Th17 cells at the site of inflammation, and relief of the disease model by removal of pathogenic Th17 cells using anti-OX40 and GITR. Further validation of pathogenic Th17 cells was not applicable, as no lineage-specific transcription factor was discovered.

Targeting pathogenic Th17 cells with specific markers has a few advantages in the treatment of Th17 cell-associated diseases. Anti-IL-17 antibodies, including ixekizumab and secukinumab, are actively used for the treatment of patients with psoriasis, patients with psoriatic arthritis, and patients with AS. For the treatment of AS patients, anti-IL-17 was the second biologic

agent approved after anti-TNF antibodies, overcoming the failures of clinical trials using other targeted agents, including anti-IL-6, CTLA-4Ig, and anti-CD20, which were successfully approved for the treatment of patients with RA (46–48). However, there have been a few concerns regarding the safety of treatment with anti-IL-17A, such as fungal infection and aggravation of intestinal inflammation (49,50). By targeting pathogenic Th17 cells using anti-OX40 and GITR, we could specifically reduce pathogenic Th17 cells with less of an impact on IL-17A-associated innate immunity.

OX40 and GITR are molecules in the T cell costimulatory TNF receptor superfamily contributing to sustained T cell responses after initial TCR stimulation (51). Both TNF receptor superfamily molecules also showed Th17 cell-promoting effects in *in vivo* models of inflammatory disease. OX40 was increased in the activated Th17 cells of ovalbumin-induced uveitis, and anti-OX40L treatment suppressed inflammation (39). GITR stimulated by its ligand GITRL promoted collagen-induced arthritis by enhancing Th17 cell responses with increased ROR $\gamma$ t expression in the spleen and joints (37,38). However, the meaning of the coexpression of OX40 and GITR was not studied. Both GITRL and OX40L were elevated in AS patients, indicating that simultaneous blocking of ligand-receptor interactions may offer therapeutic benefit through targeting pathogenic Th17 cells, though GITRL was also elevated in the SF of RA patients. Molecular pathways perturbed by dual-blockade of OX40 and GITR may lead to a better understanding of our findings on the effective suppression of pathogenic Th17 cells.

In conclusion, we described pathogenic Th17 cells in the setting of AS, a human inflammatory disease with prominent activation of Th17 cells. Moreover, the specific surface markers OX40 and GITR were discovered by a single-cell transcriptome study and validated in *in vitro* and *in vivo* experiments. Though validation of our results is required in the setting of other diseases or multiple tissues, we demonstrated critical roles of pathogenic Th17 cells in the pathogenesis of AS.

## ACKNOWLEDGMENTS

Immunofluorescent images were analyzed on a confocal microscope at the Hanyang LINC3.0 Analytical Equipment Center (Seoul). We thank our laboratory members for their support and critical suggestions throughout the course of this work.

## AUTHOR CONTRIBUTIONS

All authors were involved in drafting the article or revising it critically for important intellectual content, and all authors approved the final version to be published. Dr. T. J. Kim had full access to all of the data in the study and takes responsibility for the integrity of the data and the accuracy of the data analysis.

**Study conception and design.** K. Yi, S. Jo, H. I. Lee, H. J. Kim, J. S. Lee, E. Y. Lee, T. J. Kim.

**Acquisition of data.** K. Yi, S. Jo, S. U. Kim, S. H. Lee, J. Park, J. S. Lee, E. Y. Lee, T. J. Kim.

**Analysis and interpretation of data.** K. Yi, S. Jo, W. Song, J. H. Kang, T. H. Kim, J. S. Lee, E. Y. Lee, T. J. Kim.

## REFERENCES

1. Yao Z, Painter SL, Fanslow WC, et al. Human IL-17: a novel cytokine derived from T cells. *J Immunol* 1995;155:5483–6.
2. Blaschitz C, Raffatellu M. Th17 cytokines and the gut mucosal barrier. *J Clin Immunol* 2010;30:196–203.
3. Forlow SB, Schurr JR, Kolls JK, et al. Increased granulopoiesis through interleukin-17 and granulocyte colony-stimulating factor in leukocyte adhesion molecule-deficient mice. *Blood* 2001;98:3309–14.
4. Linden A, Adachi M. Neutrophilic airway inflammation and IL-17. *Allergy* 2002;57:769–75.
5. Amadi-Obi A, Yu CR, Liu X, et al. TH17 cells contribute to uveitis and scleritis and are expanded by IL-2 and inhibited by IL-27/STAT1. *Nat Med* 2007;13:711–8.
6. Chen L, Al-Mossawi MH, Ridley A, et al. miR-10b-5p is a novel Th17 regulator present in Th17 cells from ankylosing spondylitis. *Ann Rheum Dis* 2017;76:620–5.
7. Komiyama Y, Nakae S, Matsuki T, et al. IL-17 plays an important role in the development of experimental autoimmune encephalomyelitis. *J Immunol* 2006;177:566–73.
8. Ma HL, Liang S, Li J, et al. IL-22 is required for Th17 cell-mediated pathology in a mouse model of psoriasis-like skin inflammation. *J Clin Invest* 2008;118:597–607.
9. Shen H, Goodall JC, Gaston JS. Frequency and phenotype of peripheral blood Th17 cells in ankylosing spondylitis and rheumatoid arthritis. *Arthritis Rheum* 2009;60:1647–56.
10. Kim TJ, Kim TH. Clinical spectrum of ankylosing spondylitis in Korea. *Joint Bone Spine* 2010;77:235–40.
11. Baeten D, Sieper J, Braun J, et al. Secukinumab, an Interleukin-17A Inhibitor, in Ankylosing Spondylitis. *N Engl J Med* 2015;373:2534–48.
12. Hueber W, Sands BE, Lewitzky S, et al. Secukinumab, a human anti-IL-17A monoclonal antibody, for moderate to severe Crohn's disease: unexpected results of a randomised, double-blind placebo-controlled trial. *Gut* 2012;61:1693–700.
13. Fauny M, Moulin D, D'Amico F, et al. Paradoxical gastrointestinal effects of interleukin-17 blockers. *Ann Rheum Dis* 2020;79:1132–8.
14. Roche D, Badard M, Boyer L, et al. Incidence of anterior uveitis in patients with axial spondyloarthritis treated with anti-TNF or anti-IL17A: a systematic review, a pairwise and network meta-analysis of randomized controlled trials. *Arthritis Res Ther* 2021;23:192.
15. Gordon KB, Blauvelt A, Papp KA, et al. Phase 3 trials of ixekizumab in moderate-to-severe plaque psoriasis. *N Engl J Med* 2016;375:345–56.
16. Langley RG, Elewski BE, Lebwohl M, et al. Secukinumab in plaque psoriasis—results of two phase 3 trials. *N Engl J Med* 2014;371:326–38.
17. Ghoreschi K, Laurence A, Yang XP, et al. Generation of pathogenic T(H)17 cells in the absence of TGF- $\beta$  signalling. *Nature* 2010;467:967–71.
18. Lee Y, Awasthi A, Yosef N, et al. Induction and molecular signature of pathogenic TH17 cells. *Nat Immunol* 2012;13:991–9.
19. Nistala K, Adams S, Cambrook H, et al. Th17 plasticity in human autoimmune arthritis is driven by the inflammatory environment. *Proc Natl Acad Sci U S A* 2010;107:14751–6.
20. Omenetti S, Bussi C, Metidji A, et al. The intestine harbors functionally distinct homeostatic tissue-resident and inflammatory Th17 cells. *Immunity* 2019;51:77–89.

21. Basdeo SA, Moran B, Cluxton D, et al. Polyfunctional, pathogenic CD161+ Th17 lineage cells are resistant to regulatory T cell-mediated suppression in the context of autoimmunity. *J Immunol* 2015;195:528–40.
22. Gaublomme JT, Yosef N, Lee Y, et al. Single-cell genomics unveils critical regulators of Th17 cell pathogenicity. *Cell* 2015;163:1400–12.
23. Van der Linden S, Valkenburg HA, Cats A. Evaluation of diagnostic criteria for ankylosing spondylitis: a proposal for modification of the New York criteria. *Arthritis Rheum* 1984;27:361–8.
24. Kang HM, Subramaniam M, Targ S, et al. Multiplexed droplet single-cell RNA-sequencing using natural genetic variation. *Nat Biotechnol* 2018;36:89–94.
25. Korsunsky I, Millard N, Fan J, et al. Fast, sensitive and accurate integration of single-cell data with Harmony. *Nat Methods* 2019;16:1289–96.
26. Subramanian A, Narayan R, Corsello SM, et al. A next generation connectivity map: L1000 platform and the first 1,000,000 profiles. *Cell* 2017;171:1437–52.
27. Xie Z, Bailey A, Kuleshov MV, et al. Gene set knowledge discovery with Enrichr. *Curr Protoc* 2021;1:e90.
28. Gracey E, Hromadova D, Lim M, et al. TYK2 inhibition reduces type 3 immunity and modifies disease progression in murine spondyloarthritis. *J Clin Invest* 2020;130:1863–78.
29. Appel H, Maier R, Wu P, et al. Analysis of IL-17(+) cells in facet joints of patients with spondyloarthritis suggests that the innate immune pathway might be of greater relevance than the Th17-mediated adaptive immune response. *Arthritis Res Ther* 2011;13:R95.
30. Koski JM, Saarakkala S, Helle M, et al. Power Doppler ultrasonography and synovitis: correlating ultrasound imaging with histopathological findings and evaluating the performance of ultrasound equipments. *Ann Rheum Dis* 2006;65:1590–5.
31. Machado P, Landewe R, Lie E, et al. Ankylosing Spondylitis Disease Activity Score (ASDAS): defining cut-off values for disease activity states and improvement scores. *Ann Rheum Dis* 2011;70:47–53.
32. Butler A, Hoffman P, Smibert P, et al. Integrating single-cell transcriptomic data across different conditions, technologies, and species. *Nat Biotechnol* 2018;36:411–20.
33. Stoeckius M, Hafemeister C, Stephenson W, et al. Simultaneous epitope and transcriptome measurement in single cells. *Nat Methods* 2017;14:865–8.
34. Gutierrez M, Moreno V, Heinhuis KM, et al. OX40 agonist BMS-986178 alone or in combination with nivolumab and/or ipilimumab in patients with advanced solid tumors. *Clin Cancer Res* 2021;27:460–72.
35. Zappasodi R, Sirard C, Li Y, et al. Rational design of anti-GITR-based combination immunotherapy. *Nat Med* 2019;25:759–66.
36. Huang L, Wang M, Yan Y, et al. OX40L induces helper T cell differentiation during cell immunity of asthma through PI3K/AKT and P38 MAPK signaling pathway. *J Transl Med* 2018;16:74.
37. Tang X, Tian J, Ma J, et al. GITRL modulates the activities of p38 MAPK and STAT3 to promote Th17 cell differentiation in autoimmune arthritis. *Oncotarget* 2016;7:8590–600.
38. Wang S, Shi Y, Yang M, et al. Glucocorticoid-induced tumor necrosis factor receptor family-related protein exacerbates collagen-induced arthritis by enhancing the expansion of Th17 cells. *Am J Pathol* 2012;180:1059–67.
39. Zhang Z, Zhong W, Hinrichs D, et al. Activation of OX40 augments Th17 cytokine expression and antigen-specific uveitis. *Am J Pathol* 2010;177:2912–20.
40. Ruutu M, Thomas G, Steck R, et al.  $\beta$ -glucan triggers spondylarthritis and Crohn's disease-like ileitis in SKG mice. *Arthritis Rheum* 2012;64:2211–22.
41. Hashimoto M, Hirota K, Yoshitomi H, et al. Complement drives Th17 cell differentiation and triggers autoimmune arthritis. *J Exp Med* 2010;207:1135–43.
42. Hirota K, Hashimoto M, Yoshitomi H, et al. T cell self-reactivity forms a cytokine milieu for spontaneous development of IL-17+ Th cells that cause autoimmune arthritis. *J Exp Med* 2007;204:41–7.
43. Ciofani M, Madar A, Galan C, et al. A validated regulatory network for Th17 cell specification. *Cell* 2012;151:289–303.
44. Annunziato F, Cosmi L, Santarlasci V, et al. Phenotypic and functional features of human Th17 cells. *J Exp Med* 2007;204:1849–61.
45. Lee YK, Turner H, Maynard CL, et al. Late developmental plasticity in the T helper 17 lineage. *Immunity* 2009;30:92–107.
46. Sieper J, Porter-Brown B, Thompson L, et al. Assessment of short-term symptomatic efficacy of tocilizumab in ankylosing spondylitis: results of randomised, placebo-controlled trials. *Ann Rheum Dis* 2014;73:95–100.
47. Song IH, Heldmann F, Rudwaleit M, et al. Treatment of active ankylosing spondylitis with abatacept: an open-label, 24-week pilot study. *Ann Rheum Dis* 2011;70:1108–10.
48. Nocturne G, Dougados M, Constantin A, et al. Rituximab in the spondyloarthropathies: data of eight patients followed up in the French Autoimmunity and Rituximab (AIR) registry. *Ann Rheum Dis* 2010;69:471–2.
49. Schreiber S, Colombel JF, Feagan BG, et al. Incidence rates of inflammatory bowel disease in patients with psoriasis, psoriatic arthritis and ankylosing spondylitis treated with secukinumab: a retrospective analysis of pooled data from 21 clinical trials. *Ann Rheum Dis* 2019;78:473–9.
50. Van de Kerkhof PC, Griffiths CE, Reich K, et al. Secukinumab long-term safety experience: a pooled analysis of 10 phase II and III clinical studies in patients with moderate to severe plaque psoriasis. *J Am Acad Dermatol* 2016;75:83–98.
51. Watts TH. TNF/TNFR family members in costimulation of T cell responses [review]. *Annu Rev Immunol* 2005;23:23–68.